THE ASTROPHYSICAL JOURNAL, 503:831–842, 1998 August 20
© 1998. The American Astronomical Society. All rights reserved. Printed in U.S.A.

SOFT X-RAY SCATTERING AND HALOS FROM DUST

RANDALL K. SMITH[1] AND ELI DWEK
NASA Goddard Space Flight Center, Code 685, Greenbelt, MD 20771
Received 1997 October 22; accepted 1998 March 27

ABSTRACT

Small-angle scatterings of X-rays by interstellar dust particles create halos around X-ray sources. The halo intensity and its projected radial distribution around a source can provide important information on the spatial distribution of the dust along the line of sight to the source and on the physical properties of the scattering dust particles. Halos around X-ray point sources have been used by several authors to infer that the scattering dust particles are fluffy in nature, consisting of aggregates of smaller refractory particles with vacuum occupying a significant fraction of their volume. The nature and morphology of interstellar dust particles has recently gained new importance, since fluffy, composite dust particles have been suggested as a possible solution to the interstellar carbon "crisis." This crisis results from the discrepancy between the abundance of carbon in the interstellar medium available for creating dust and the significantly larger amount of carbon that must be in dust in order to account for the UV-optical interstellar extinction in the diffuse ISM. Previous studies of X-ray scattering have used the Rayleigh-Gans (RG) approximation to the differential scattering cross section to calculate halo properties. However, the validity of the RG approximation fails for energies below 1 keV. We use the exact Mie solution for the differential scattering cross section and find that, for these energies, the scattering becomes much less efficient than is predicted by the RG approximation. Furthermore, the effects of K and L shell absorption by atoms in the dust become important. The net effect is that the RG approximation systematically and substantially overestimates the intensity of the halo below 1 keV, relative to the Mie solution result. In particular, Mathis and coworkers used the weaker than expected halo intensity observed around Nova Cygni 1992 to conclude that interstellar dust must be fluffy. Using the Mie solution to the scattering intensity and including the effects of absorption, we find that, contrary to the conclusion of Mathis and coworkers, the halo around Nova Cygni 1992 does not *require* interstellar dust grains to be fluffy in nature and that the data are consistent with scattering from a mixture of bare refractory silicate and carbon grains as well.

Subject headings: dust, extinction — ISM: abundances — novae, cataclysmic variables — stars: individual (Nova Cygni 1992) — X-rays: general — X-rays: ISM

1. INTRODUCTION

Measuring the small-angle scattering of X-rays from particles embedded in a uniform medium to calculate their size and shape has long been a standard technique in microbiology (Glatter & Kratky 1982). In the laboratory, small-angle X-ray–scattering observations can measure the size and shape of the scattering particles quite accurately, but astrophysical applications are still sharply limited by the availability of sufficiently bright X-ray sources and the spatial and energy resolution of X-ray telescopes. The scattering of X-rays from dust grains in the interstellar medium (ISM) was first considered by Overbeck (1965). However, the weak X-ray halo generated by small-angle X-ray scattering from dust has only recently become observable (Mauche & Gorenstein 1986, hereafter MG86; Predehl & Schmitt 1995). Recent observations using the *ROSAT* Position Sensitive Proportional Counter (PSPC; Predehl & Schmitt 1995) have found X-ray halos around 25 point sources and 4 supernova remnants, using the moderate 25″ resolution of this instrument. The *Advanced X-Ray Astrophysical Facility* (*AXAF*) telescope will have a compact point-spread function (~1″ FWHM) and a low detector background (Canizares 1990), and it should dramatically increase the number of sources with visible halos.

The halo formed around an X-ray point source by small-angle scattering depends, in addition to the spatial distribution of the dust, upon many details of the interstellar dust grain population. In the general case this is a radiative transfer problem, and the halo intensity is proportional to $\exp(-\tau)$, where $\tau \propto N_g$, the column density of grains along the line of sight. We will consider the limit where singly scattered X-rays dominate the halo, in which case the intensity varies linearly with N_g. The halo is highly dependent upon the size distribution of the larger grains, which more efficiently scatter X-rays. A population of spherical dust grains scatter X-rays with an angular distribution determined by the grain size distribution, composition, and density. Given these dust parameters, the spatial distribution of the grains can be estimated by comparing this scattered distribution with the observed halo. Although it is difficult to extract each dust grain parameter separately, measurements of the halo intensity as a function of energy and angle from the source can provide useful limits on the allowable dust grain model parameters.

The general theory of X-ray scattering by dust grains has been discussed in detail by MG86 and Mathis & Lee (1991, hereafter ML91). Their results were based on the Rayleigh-Gans (RG) approximation to the differential scattering cross section. Predehl & Klose (1996, hereafter PK96) discussed the possibilities for extracting dust grain parameters by observing X-ray halos with current X-ray telescopes. They also considered the limitations of the RG approx-

[1] Current address: High Energy Astrophysics Division, Smithsonian Astrophysical Observatory, 60 Garden Street, Cambridge, MA 02138.

imation and the effects of absorption in the dust grain on the scattered X-rays. Recent observations of X-ray halos (Mathis et al. 1995, hereafter MCFK95; Woo et al. 1994; Predehl 1996), using both the *ROSAT* and *ASCA* telescopes, have found that the observed halo intensity is less than that predicted by the general theory using the RG approximation. These authors concluded that their results were evidence for "fluffy" dust grains, which contain many holes and voids.

These results are of particular interest because of the carbon "crisis" in the ISM (Cardelli et al. 1996). Observations have suggested that the amount of carbon available to be in dust grains is substantially less than the amount necessary to make the grains that account for the observed extinction. Mathis (1996, hereafter M96) has suggested that fluffy dust grains would account for the extinction measurements while reducing the amount of carbon necessary to be locked up in the dust.

However, Dwek (1997) pointed out that the composite fluffy dust model (CFD) suggested by Mathis fails to resolve the interstellar carbon crisis for several reasons. First, the visual albedo of the CFD particles is lower than that observed. The increased absorptivity of the composite dust grains therefore produces an excess of infrared emission over that observed with the Diffuse Infrared Background Experiment (DIRBE) and Far Infrared Absolute Spectrophotometer (FIRAS) instrument onboard *COBE* (Dwek et al. 1997). Secondly, the CFD model does not include polycyclic aromatic hydrocarbons (PAHs) as a grain constituent. As a result, it does not take the abundance of carbon locked up in PAHs or the effect of PAHs on the UV and optical extinction into account. In light of these difficulties, we reexamine the theory of X-ray scattering by interstellar dust particles and the evidence for the existence of CFD particles in the ISM.

We present in § 2 a brief review of the theory, describing the RG approximation to the X-ray scattering from a spherical particle, and examining the range of its validity. In § 3 we present the exact Mie solution to light scattering from a spherical particle and describe the differences between the Mie theory and the RG approximation for various astrophysical situations, including the importance of absorption of X-rays in the dust. In § 4 we apply the Mie theory to the observations of Nova Cygni 1992 from MCFK95 and discuss the implications for dust models.

2. BASIC THEORY

The physical situation we consider is the small-angle scattering of X-rays emitted by a bright X-ray source from dust grains in the ISM near the line of sight (LOS), which will create an X-ray halo around the point source. The scattered angles are small enough that, for astronomical purposes, we can assume that the path traveled by the unscattered primary X-rays is nearly identical to the paths of scattered photons, in terms of their distances and environments. We discuss this assumption and its limitations in Appendix A.

Consider the X-ray source S (see Fig. 1), which, at distance D from the observer O, has an observed flux F_X and spectrum $S(E)$ in the (E_{min}, E_{max}) energy range, where $S(E)$ is normalized to unity over that interval. The emitted X-rays travel though the ISM and scatter from a population of dust grains with number density $n(a)da$ per H atom in the interval $(a, a + da)$ for grain radii in the range (a_{min}, a_{max}). We assume that the grain size distribution is uniform but

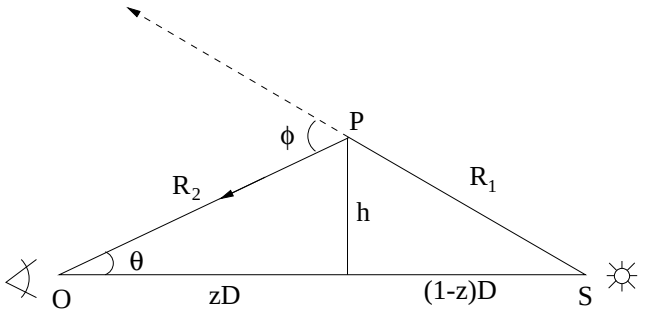


FIG. 1.—Scattering diagram of an X-ray emanating from a source S that is scattered through an angle ϕ by a dust particle located at P toward an observer O. The parameter $z \equiv R_2 \cos\theta/D$ is a dimensionless quantity denoting the projected distance to the dust particle from O along the LOS to S.

that its average number density can vary along the LOS. We characterize the spatial distribution of the grains by the function $f(z)$, where $z \equiv R/D$ is the normalized distance from the observer for an actual distance R from the observer; $f(z)$ is normalized to unity over the range (0,1). Finally, the scattered power in a given direction is determined by the differential scattering cross section $(d\sigma/d\Omega)$, which is a function of X-ray energy, dust grain size, and scattering angle.

In the most general form, we can write the equation for the scattered intensity at angle θ, in units of photons cm^{-2} s^{-1} sr^{-1}, as (see Appendix A)

$$I_{sca}(\theta) = \int_{E_{min}}^{E_{max}} dE F_X S(E) \int_{a_{min}}^{a_{max}} da N_H n(a) \times \int_0^1 \frac{f(z)}{(1-z)^2} \left[\frac{d\sigma(E, a, \phi)}{d\Omega}\right] dz \, . \quad (1)$$

Equation (1) apparently diverges for scattering near the source, where $z \to 1$. However, near the source the contribution to the flux scattered to the observer comes from relatively large scattering angles, for which $(d\sigma/d\Omega)$ is vanishingly small. So, in practice, using an upper limit $1 - \epsilon$ instead of 1 to the position integral for some small ϵ is acceptable, since the integral from $1 - \epsilon$ to 1 is negligible. Numerical experiments, with smoothly distributed dust $[f(z) \equiv 1]$, a single grain size, and a single X-ray energy, show that the integral (using the Mie solution for the scattering term) converges to within 1 part in 10^6 when $\epsilon \equiv \theta$ (measured in radians). This conclusion holds for dust sizes in the range 0.1–1.0 μm and X-ray energies in the range 0.1–1.0 keV. Using this result, we can modify equation (1) by changing the upper limit on z to be $1 - \theta$, so that

$$I_{sca}(\theta) = F_X N_H \int_{E_{min}}^{E_{max}} dE S(E) \int_{a_{min}}^{a_{max}} da n(a) \times \int_0^{1-\theta} \frac{f(z)}{(1-z)^2} \left(\frac{d\sigma}{d\Omega}\right) dz \, , \quad (2)$$

which removes the numerical difficulties.

In addition, as stated in § 1, in this paper we consider only singly scattered X-rays. Although ML91 developed the theory of multiply scattered X-ray halos, the brightest X-ray halos occur when the optical depth to scattering is low, $\tau_{sca} \sim 0.2$ (PK96). PK96 also found that when the optical depth for scattering was high enough that multiple scattering was important, absorption along the LOS greatly reduced both the source and halo intensity.

2.1. *Rayleigh-Gans Theory*

The RG approximation for the differential scattering cross section ($d\sigma/d\Omega$) requires the following two assumptions: First, that the reflection from the surface of the dust particle is negligible, i.e., that $|m-1| \ll 1$, where m is the complex index of refraction of the dust. This ensures that the X-ray enters the dust particle instead of being reflected. The second, more stringent requirement is that

$$k_0 a |m-1| \ll 1 , \tag{3}$$

where k_0 is the wave number of the X-ray and a the radius of the grain. This ensures that the phase of the incident wave is not shifted inside the medium. We will show how, in this limit and for sufficiently small scattering angles, it is possible for the waves scattered throughout the dust grain to add coherently. In this situation, the intensity of the scattered waves is proportional to the number of scattering sites squared; i.e.,

$$I \propto N^2 \propto \rho^2 a^6 , \tag{4}$$

where ρ is the mass density of the dust grain.

A useful limit for the RG approximation assumptions can be derived using the "Drude approximation" to $|m-1|$, which applies in the case of a collection of free electrons responding to an oscillating external field. The Drude approximation (Bohren & Huffman 1983) is

$$m \approx \sqrt{1 - \frac{\omega_p^2}{\omega^2 + i\gamma\omega}} , \tag{5}$$

where ω is the circular frequency of the wave and $\omega_p^2 = 4\pi c^2 n_e r_e$ is the plasma frequency of the medium (for electron number density n_e and where r_e is the classical radius of the electron). The γ term is a damping term due to electronic interactions with impurities or lattice vibrations. Assuming $|m-1| \ll 1$, we can rewrite equation (5) to get

$$|m-1| \approx \frac{n_e r_e \lambda^2}{2\pi}\left(\frac{1}{1 + i\gamma/\omega}\right), \tag{6}$$

where λ is the wavelength of the photon. Combining equation (6) with equation (3) and ignoring damping (i.e., $\gamma = 0$), we get

$$a n_e r_e \lambda \ll 1 . \tag{7}$$

Equation (7) can be expressed in terms of the dust mass density ρ by assuming that the atomic constituents of the dust have one electron for every two nucleons, so $n_e = \rho/(2m_{\rm H})$. The coherency requirement for the validity of the RG approximation then becomes

$$\frac{a_{\mu\rm m}}{E_{\rm keV}}\left(\frac{\rho}{3\ \rm g\ cm^{-3}}\right) \ll 0.316 . \tag{8}$$

A "rule of thumb," then, for normal interstellar dust grains is that the RG approximation is valid only if the energy of the X-ray in keV is significantly larger than the grain radius in μm.

Within this limit, the RG approximation completely describes the scattering of photons in a simple analytic form. The exact RG approximation for the differential scattering cross section is given in MG86 and shown below. The exact result is in terms of the spherical Bessel function j_1 but can be well approximated by a Gaussian function:

$$\left(\frac{d\sigma}{d\Omega}\right)(E, a, \phi) = 2a^2\left(\frac{2\pi a}{\lambda}\right)^4 |m-1|^2\left[\frac{j_1(y)}{y}\right]^2(1 + \cos^2\phi) \tag{9}$$

$$\approx 2a^2\left(\frac{2\pi a}{\lambda}\right)^4 |m-1|^2 \frac{1}{9}\exp\left(-\frac{y^2}{2\sigma^2}\right)(1 + \cos^2\phi) , \tag{10}$$

where $y = (4\pi a/\lambda)\sin(\phi/2)$, and σ is a function of the energy and size of the dust particle. We see here the a^6 dependence described earlier; the ρ^2 dependence is implicit in the $|m-1|^2$ term (see eq. [6]).

Insight into the mechanism and the maximum angle for coherent scattering can be derived from the fundamental physics of the scattering. Photons scatter from charged particles, and the differential scattering cross section for photons interacting with a collection of charged free particles is given by Jackson (1975; see that book eq. [14.111]):

$$\frac{d\sigma}{d\Omega} = \left|\sum_j \frac{e_j^2}{m_j c^2} e^{i\boldsymbol{q}\cdot\boldsymbol{r}_j}\right|^2 |\boldsymbol{\epsilon}^* \cdot \boldsymbol{\epsilon}_0|^2 , \tag{11}$$

where the sum is taken over all the charges in the medium. Here e_j is the charge of the jth particle, m_j is its mass, and $\boldsymbol{r}_j$ is its position relative to the center of the dust particle (see Fig. 2). We define $\boldsymbol{q} \equiv (\omega\hat{\boldsymbol{n}}_s - \omega_0\hat{\boldsymbol{n}}_i)/c$, where $\hat{\boldsymbol{n}}_i$ and $\hat{\boldsymbol{n}}_s$ are unit vectors in the initial and scattered directions, respectively, ω_0 and ω are the circular frequencies of the X-ray outside and inside the medium, respectively, and c is the speed of light. The initial and scattered polarization is given by $\boldsymbol{\epsilon}_0$ and $\boldsymbol{\epsilon}^*$, respectively; however, we will not consider X-ray polarization in this paper and will therefore ignore these terms.

We see immediately that effectively all the scattering is by electrons; scattering by protons is strongly suppressed because of their large mass. Figure 2 diagrams the situation for one particular scattering site in a spherical dust grain.

Equation (11) is strictly valid only for free electrons. However, X-rays are substantially more energetic than the electronic energy bands in the solids, so the electrons in the dust grain can be treated as free (Jackson 1975). Absorption, however, is not entirely negligible, even above 1 keV,

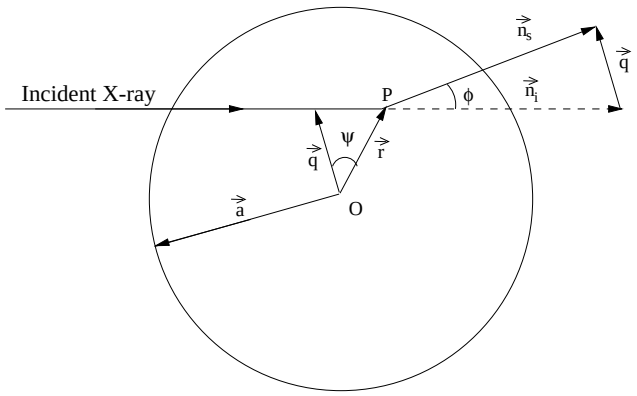


FIG. 2.—X-ray traveling in direction $\boldsymbol{n}_i$, impinging upon a dust particle of radius a, interacting at a point P located at a distance r from the center of the particle O, and scattering in the direction $\boldsymbol{n}_s$.

because there are a number of elements with K-shell electrons that can absorb at these energies (see § 3.2).

We can now show how to derive the limiting angle for coherent scattering. If $|\boldsymbol{q}\cdot\boldsymbol{r}_j| \ll 1$ in equation (11), the exponent term reduces to unity. Then the sum is simply $[Ne^2/(m_e c^2)]^2$, where N is the total number of electrons in the dust grain. Physically, this result is due to each electron scattering independently and the resulting waves adding coherently. The intensity, therefore, is a function only of the *number* of electrons in the scattering medium and not of the *spacing* or *density* of the electrons.

Expanding terms in $|\boldsymbol{q}\cdot\boldsymbol{r}_j| \ll 1$, we get, using the notation of Figure 2,

$$\begin{aligned}|\boldsymbol{q}\cdot\boldsymbol{r}| &= \left|\left(\frac{\omega}{c}\,\hat{\boldsymbol{n}}_s - \frac{\omega_0}{c}\,\hat{\boldsymbol{n}}_i\right)\cdot\boldsymbol{r}\right| \\ &= \left|\left(\frac{\omega}{c}\,\hat{\boldsymbol{n}}_s - \frac{\omega_0}{c}\,\hat{\boldsymbol{n}}_i\right)\right|\cdot|\boldsymbol{r}||\cos\psi| \\ &= \left[\left(\frac{\omega}{c}\right)^2 + \left(\frac{\omega_0}{c}\right)^2 - 2\,\frac{\omega\cdot\omega_0}{c^2}\,\hat{\boldsymbol{n}}_s\cdot\hat{\boldsymbol{n}}_i\right]^{1/2} r|\cos\psi|\,.\end{aligned} \tag{12}$$

The complex optical constant for the dust grain relates ω and ω_0 via $\omega = m\omega_0$. Substituting in equation (12) we get

$$|\boldsymbol{q}\cdot\boldsymbol{r}| = k_0(m^2 + 1 - 2m\cos\phi)^{1/2} r|\cos\psi|\,, \tag{13}$$

where $k_0 = \omega_0/c$. The position vector $\boldsymbol{r}$ takes on all values between $0 < r < a$, where a is the radius of the dust, and $0 < |\cos\psi| < 1$. Replacing $r|\cos\psi|$ with its maximum value, a, the requirement that $|\boldsymbol{q}\cdot\boldsymbol{r}| \ll 1$ becomes

$$|(m^2 + 1 - 2m\cos\phi)|^{1/2} k_0 a \ll 1\,. \tag{14}$$

Note that equation (14) is equivalent to equation (3) for $\phi \to 0$, so if the RG assumptions are met, coherent scattering will occur for at least some scattering angles. We can rewrite equation (14) using some trigonometry and the already-stated assumption that $|m - 1| \ll 1$ to get a better limit on the scattering angle:

$$2k_0 a \sin\left(\frac{\phi}{2}\right) \ll 1\,. \tag{15}$$

In the X-ray regime, $k_0 \sim 5000 E_{\rm keV}\ \mu{\rm m}^{-1}$. Thus $k_0 a$ will be much larger than unity for normal interstellar dust grains and $\sim$1 keV X-rays, so we can use the small angle approximation for sin $(\phi/2)$. Waves scattered at angles where $\phi \ll 1/k_0 a$, when the RG assumptions are met, will have intensities proportional to N^2, the number of electrons in the grain squared.

To summarize, the RG approximation requires that the dust neither reflects photons nor significantly affects their phases. The induced scattering wave generated at the entrance to the grain must add in phase with one created at the exit. If it does not, then coherency is lost, and the amplitude of the scattered wave never becomes proportional to the number of electrons squared in the entire dust volume squared, but only to a fraction of that number.

Furthermore, the combination of the RG approximation with the Drude approximation assumes that absorption is negligible at all energies. This is approximately valid when $E > 1$ keV, although there are astronomically abundant elements in dust with atomic energy levels above 1 keV, e.g., magnesium (K edge, 1.294 keV), aluminum (K edge, 1.550 keV), silicon (K edge, 1.828 keV), and iron (K edge, 7.083 keV). Below 1 keV, however, there are many elements whose K and L shell edges can absorb X-rays, an effect which will be considered in § 3.2. The breakdown of the RG approximation and the effect of absorption requires the use of full Mie theory to correctly calculate the intensity of the scattered light.

3. MIE THEORY

Mie theory calculates the exact solution for the scattering and absorption of light from a spherical particle (van de Hulst 1957). Unlike the RG approximation, it does not assume all the scattering sites will add coherently, and, as a result, Mie theory can correctly calculate the scattered intensity for particles even when $a_{\mu\rm m} \gtrsim E_{\rm keV}$. In the limit where $k_0 a|m - 1| \ll 1$, the Mie solution recovers the result of the RG approximation. Another advantage is that absorption can be easily included, using measured values for the index of refraction. However, although the Mie solution is exact for light scattering from a sphere, unlike the RG approximation it is not expressible in a useful analytic form.

The Mie solution requires careful numerical computation, especially for large values of the "size parameter" $x \equiv 2\pi a/\lambda \approx 5000 a_{\mu\rm m} E_{\rm keV}$, where the series solution requires summation over a large number of terms to converge. We use the Mie code developed by Wiscombe (1979, 1980), which was written for atmospheric use but has been tested for size parameters up to 20,000, sufficient for our problem. The observed scattered intensity is obtained by integrating the intensity of the light scattered by a single dust particle to the observer, over the grain size and spatial distribution along the LOS (see eq. [A4] in the Appendix). These calculations can be greatly facilitated by precalculating tables of $[d\sigma(E, a, \phi)/d\Omega]$ for a range of energies, dust sizes, and scattering angles.[1]

We must point out, however, that even the Mie solution is only of an approximate nature, since dust particles are neither spherical nor compositionally homogeneous. We know that the first assumption is incorrect, since only nonspherical grains can polarize light, as grains have been observed to do (e.g., Mathis 1990). The second assumption is particularly important, since the wavelength of a 1 keV photon is only 1.24 Å, substantially smaller than the radius of any dust grain. Thus, the X-ray's path through the grain will determine which dust grain constituents it interacts with, and so the X-ray scattering will be affected by the grain's exact morphology. Exploring this possibility in detail would require a discrete dipole approximation to the dust grain constituents (e.g., Draine 1988), which is beyond the scope of this paper.

3.1. *Comparison to the Rayleigh-Gans Approximation*

The observed halo intensity can be calculated for any X-ray energy and dust grain size, using either RG approximation or the Mie solution. Any variation in the result is due solely to the differential scattering cross section $(d\sigma/d\Omega)$ term. In Figure 3 we plot $(dQ_{\rm sca}/d\Omega) \equiv (d\sigma/d\Omega)/\pi a^2$ for 2

[1] The code needed to generate such tables and related utilities may be obtained from the first author.

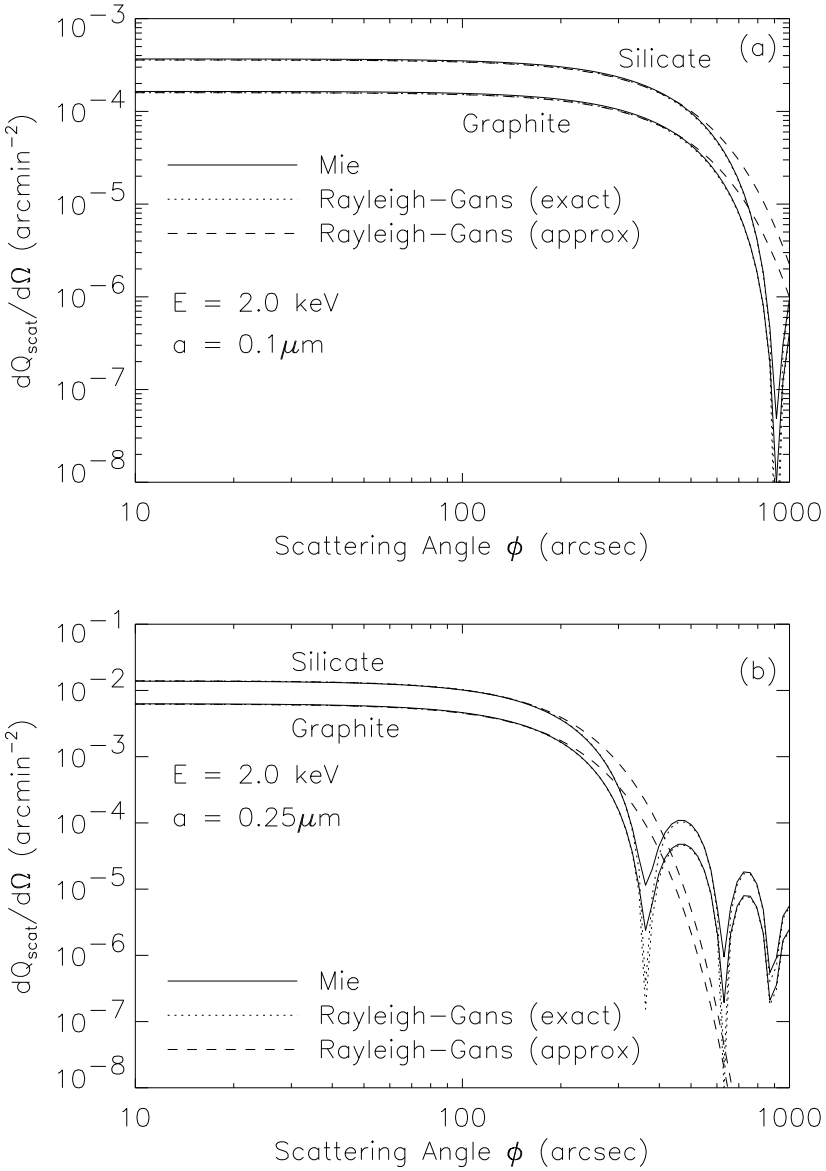


FIG. 3.—(*a*) Differential scattering cross sections $dQ_{sca}/d\Omega = (d\sigma/d\Omega)/\pi a^2$, for a 2 keV X-ray scattering from a 0.1 μm dust grain, for both graphite and silicate dust grains. The solid lines show the Mie calculation, using the Drude approximation to the optical constants. The exact RG result is shown with the dotted lines, and the dashed lines show Gaussian approximation to the RG result. In this energy and ϕ range, the three methods should give identical results. Note that the use of the Gaussian approximation leads to deviations at large angles. (*b*) Same as (*a*) but for 0.25 μm dust grains.

keV X-rays scattering from a single dust grain, as a function of the scattering angle ϕ. The differential scattering cross section was divided by the geometrical cross section to show the relative effect of grain size on the scattering intensity. Figure 3*a* presents the results for both a graphite or silicate dust grain of radius 0.1 μm, and Figure 3*b* is similar but for grains of size 0.25 μm. The mass densities of the two types of dust, graphite and silicate, were 2.2 and 3.3 g cm^{-3}, respectively. The optical constants were calculated using the Drude approximation, ignoring absorption, for both the RG and the Mie cases, so that the variation in the figures is due solely to the approximate nature of the RG solution.

Figure 3 shows that at 2 keV the Gaussian approximation to the Bessel function in the RG approximation is adequate; it deviates substantially from the exact RG and the Mie solution only at large angles, after the scattering intensity has dropped substantially. The deviation itself is largely due to the Gaussian approximation.

When the requirement that $k_0 a|m-1| \ll 1$ is not satisfied, the agreement between the RG and the Mie solution becomes substantially worse. Figure 4 is identical to Figure 3 but for X-rays of energy 0.5 keV. The "rule of thumb" suggests that, in this case, the RG approximation will hold for 0.1 μm radius dust but fail for the 0.25 μm radius dust. Figure 4 confirms this, showing an acceptable match between the RG and the Mie calculations for the smaller grains, but showing far more total scattering with the RG approximation than in the Mie solution for the larger grain size. In this case, using the exact Bessel function solution does not help. The larger dust grain has more scattering sites, and the RG approximation assumes all the scattered waves all add coherently; the Mie solution shows that for large dust sizes this coherency assumption fails, and the scattered intensity therefore drops. Figure 4 suggests that the approximation fails abruptly, as might be predicted from the exponential nature of equation (11).

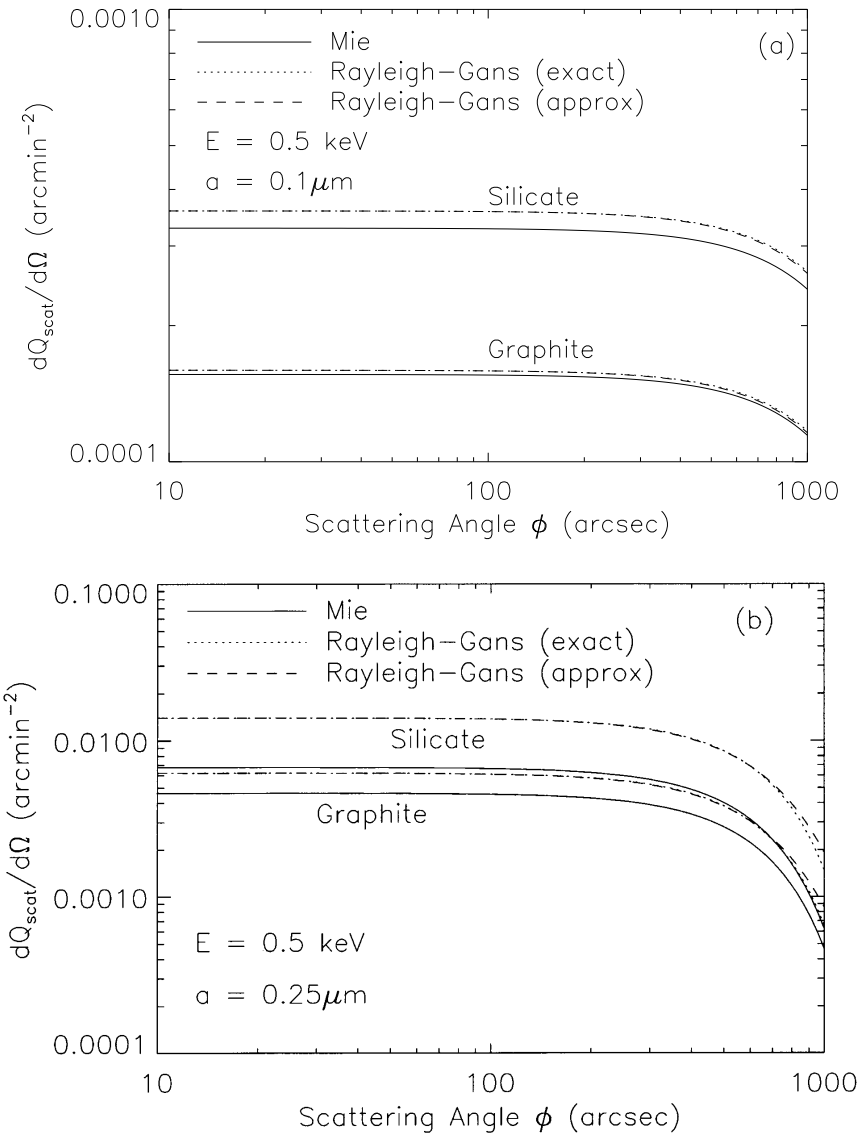


FIG. 4.—(*a*) Same as Fig. 3 but for 0.5 keV X-rays. Both RG results agree with each other and are acceptably close to the Mie calculations. (*b*) Same as (*a*) but for a 0.25 μm dust grain. The assumptions necessary for the RG approximation do not hold, and the results show that the differential scattering cross sections calculated using the Mie and RG approximation disagree substantially at all scattering angles, although the two RG methods agree with each other.

3.2. *The Effect of Absorption*

We have so far used the Drude approximation to the optical constants, ignoring any damping, in both the RG approximation and the Mie solution. Although the Drude approximation works well above 1 keV, real dust grain constituents have many K and L shell electrons with energy levels that are in the range 0.1–1 keV, and these electrons will absorb soft X-rays. The effect of absorption can be included by using the atomic scattering factor $F(E)$ (Henke 1981) as a modifier to the Drude approximation:

$$|m-1| = \frac{n_e r_e \lambda^2}{2\pi}\left|\frac{F(E)}{Z}\right|, \qquad (16)$$

where Z is the atomic number of the element. However, we simply use the measured optical constants, which include the absorption effects. For silicate particles ($\{MgFeSi\}O_4$) we used the optical constants of Martin & Rouleau (1991), and for graphite particles we used Rouleau & Martin (1991). These values are a smooth extension of the Draine & Lee (1984) results into the far-UV and X-ray regime. At X-ray energies, there is no distinction between graphite and amorphous carbon, so this complication need not be considered. We also considered composite dust particles as described in M96; for this case, we used the Bruggeman rule (Bohren & Huffman 1983) to calculate the optical constants of the mixture.

Figure 5*a* plots the observed halo intensity for 2 keV X-rays and a distribution of grain sizes, calculated three different ways. We presented the observed halo rather than showing $(d\sigma/d\Omega)$ for a single dust grain size, as was shown in Figures 3 and 4, to show the magnitude of the observable differences between the methods. For 2 keV X-rays, these differences are clearly small. The halo intensity, given by equation (1), was found by integrating $(d\sigma/d\Omega)$ over a spatially even distribution of dust particles $[f(z) \equiv 1]$ charac-

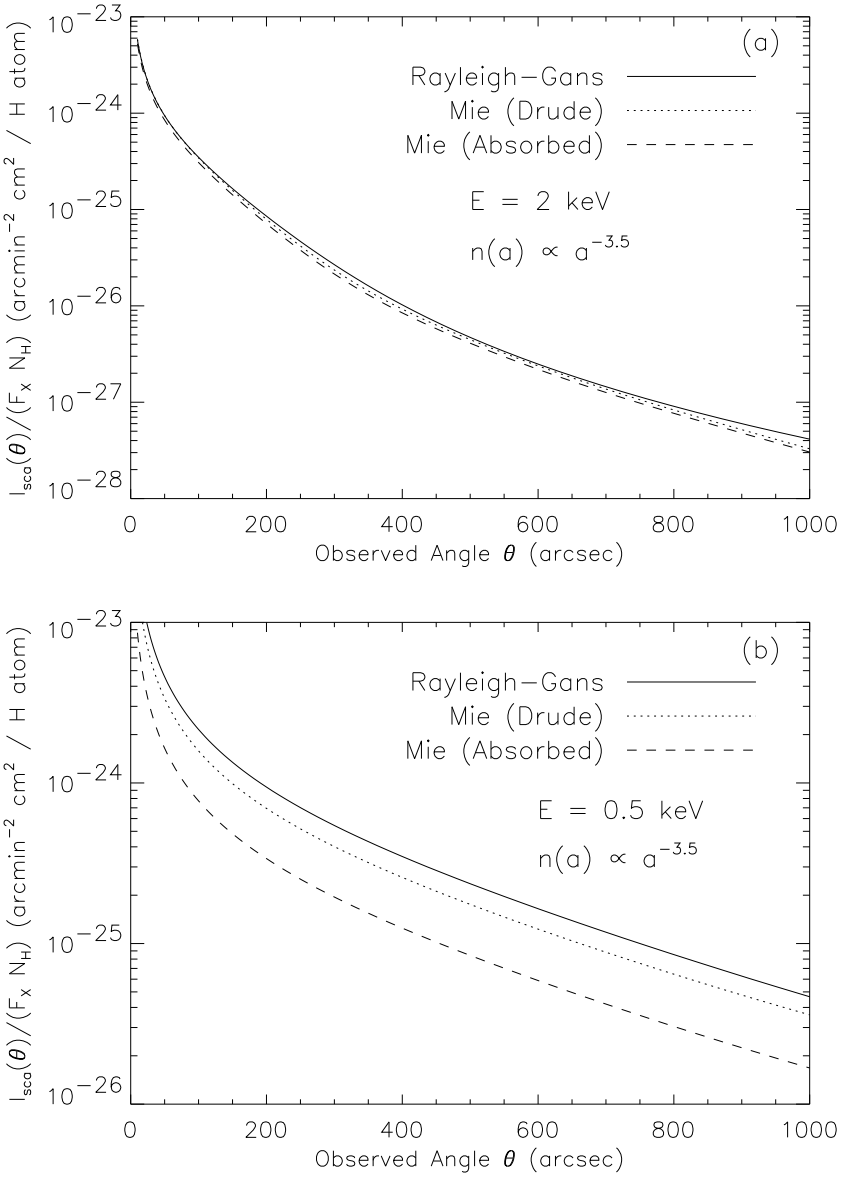


FIG. 5.—(*a*) Observed halo intensity from a 2 keV X-ray source scattering from a spatially uniform distribution of silicate and graphite dust grains, both with an $n(a) \propto a^{-3.5}$ size distribution. The results are shown using the RG approximation, the Mie solution with the Drude approximation to the index of refraction (i.e., without absorption), and the Mie solution using measured optical constants. (*b*) Same as (*a*) but for 0.5 keV.

terized by a size distribution $n(a) \propto a^{-3.5}$, with $(a_{\min}, a_{\max}) = (0.005\ \mu\text{m}, 0.25\ \mu\text{m})$. The grains themselves consisted of a mix of silicate and graphite grains with dust-to-hydrogen mass ratios of 0.0057 and 0.0032, respectively.

We note that the choice of the upper limit to the size distribution, 0.25 μm, significantly affects the result. With this power-law size distribution, most of the mass is in the largest grains. In addition, the distribution of the largest dust particles are not well determined by extinction measurements, because when the grain size is much larger than the wavelength, the extinction becomes independent of wavelength. X-ray halos are therefore a particularly useful and sensitive probe of the number and size of large dust grains. In the RG approximation, the intensity is proportional to the sixth power of the radius of the dust. The Mie solution also predicts larger dust grains scatter more than small grains, although not by as large a power (see Figs. 4*a* and 4*b*). In general, however, the source function of the scattered intensity is heavily weighted toward large dust grains.

Figure 5 shows the cumulative effects of the approximations used in calculating the observed halo intensity. The simple RG approximation (with the Gaussian fit to the Bessel function and the Drude approximation to the optical constants) predicts the largest intensity. The exact Mie solution, using the Drude approximation, reduces the intensity, since not all the scattered waves add coherently. The Mie solution, using actual optical constants that include absorption, has the lowest intensity, since some of the impinging X-rays are absorbed in the dust.

The effect of absorption can be much larger; this is shown in Figure 5*b*, which is identical to Figure 5*a* but for 0.5 keV X-rays. The difference between the RG and the Mie solution for a realistic dust grain size distribution is quite noticeable, and Figure 5*b* shows that absorption is very important at this energy. We note in passing that not all of the X-ray's

energy must be deposited in the dust (Dwek & Smith 1996), since the ejected photoelectron may exit the grain and deposit only a fraction of its energy in the solid.

We have shown that the accuracy of the RG approximation is size dependent and is, in general, less accurate at larger grain sizes. The interstellar grain population is characterized by a mixtures of grain sizes, and it is therefore interesting to apply Mie theory to an astronomical situation.

3.3. *The Energy Dependence*

In Figure 6, both the Mie and RG methods were used to calculate the intensity of scattered X-rays from silicate grains as a function of X-ray energy, at the observed scattering angle $\theta = 100''$. For this comparison, we assumed that the dust grain size distribution was a delta function and considered both 0.1 μm and 0.25 μm grain radii. We see that for higher energies, the shape of the curves for the two methods begins to agree when $E \gtrsim 1$ keV, but below this energy there are substantial differences. The two methods never agree exactly because of absorption, which is more important for larger grains but is not negligible, even for the 0.1 μm grain. The presence of absorption lines in the grains can also be seen in the halo shape, which has irregular peaks and valleys in the Mie case.

We conclude that, in many astronomical situations, using the RG approximation to calculate the halo intensity systematically overestimates the amount of X-ray scattering from a given dust size distribution. Consequently, the RG approximation cannot be used for X-ray energies below 1 keV, except as an upper limit to the halo intensity. Even for energies above 1 keV, RG is only an upper limit, since absorption is never totally negligible and will reduce the total intensity of scattered light.

4. APPLICATION AND DISCUSSION

The total scattered light intensity will in practice depend upon the spectrum of the source $S(E)$, the spatial distribution of dust grains $f(z)$, and the grain size distribution $n(a)$. We can measure the X-ray spectrum $S(E)$ directly, and we will assume that the dust grains have a spatially even distribution, so that $f(z) \equiv 1$. The last parameter, the dust grain size distribution $n(a)$, is not well known, especially for larger size grains. Currently, it is measured by fitting the extinction of visible and UV starlight. We will present results using two different grain models: (1) a bare core silicate and graphite mix, with an $a^{-3.5}$ power-law size distribution (following Mathis, Rumpl, & Nordsieck 1977, hereafter MRN); and (2) the recent CFD model of M96, a distribution centered near 0.1 μm consisting of composite silicate and graphite. We now apply the RG and Mie solutions with these grain models to the observed scattering from the X-ray source (Nova Cygni 1992).

4.1. *Nova Cygni 1992*

Nova Cygni 1992 exhibited a strong X-ray halo in the *ROSAT* PSPC (MCFK95). The observed spectrum was formally fitted with a blackbody with temperature $E = kT \sim 22$ eV, absorbed by an equivalent hydrogen column density of $N_{\rm H} = 4.25 \times 10^{21}$ cm^{-2}. This is not an accurate model of the nova, but it is simple to calculate and fits the observed spectrum reasonably well. The observed spectrum peaked at about 0.5 keV; most of the photons from the source were absorbed. However, this column density is not the best choice for use in the scattering-intensity equation (1), since the value of $N_{\rm H}$ is highly dependent upon the actual spectrum of the source. In addition, the hydrogen column density measured from X-ray absorption depends upon the column density of helium and metals along the LOS and is not directly related to the column density of dust grains along the LOS. Therefore, X-ray absorption measures of the hydrogen column density may not accurately reflect either the actual hydrogen column density or the dust grain column density.

In the single-scattering limit, the scattered halo intensity scales linearly with the column density of dust grains, which

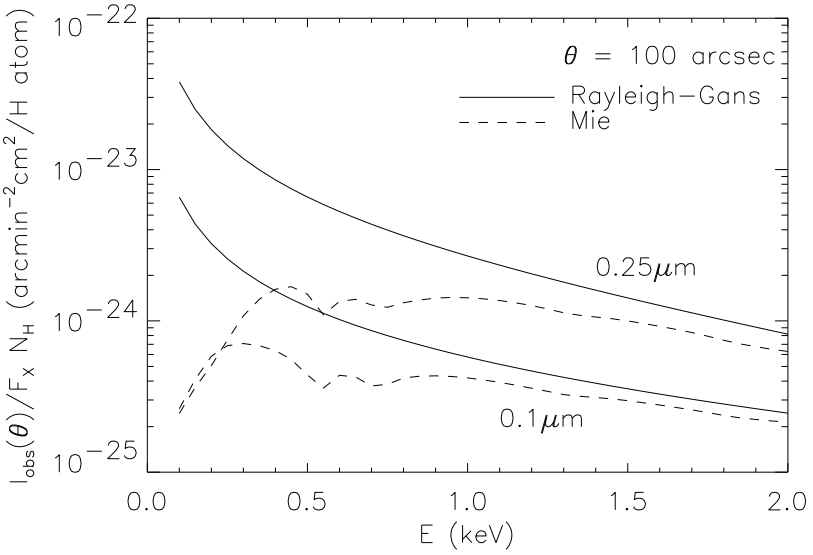


FIG. 6.—Scattered intensity at 100″ for silicate grains of radius 0.1 and 0.25 μm, calculated both by the RG approximation (without absorption) and the Mie solution (including absorption) as a function of X-ray energy. For $E \gtrsim 1$ keV, the two methods show the same energy dependence; below it, absorption modifies the E dependence, an effect that becomes more pronounced at 0.25 μm.

TABLE 1

DUST GRAIN PARAMETERS

Model	Component	$n(a)$	ρ (g cm^{-3})	C/H (ppm)	Si/H (ppm)	$f_{\rm vacuum}$
MRN[a]	Graphite	$a^{-3.5}$	2.2	270	0	0
	Silicate	$a^{-3.5}$	3.3	0	33	0
CFD[b]	Graphite	$\ll 0.03$ μm	2.25	55	0	0
	Silicate	$\ll 0.02$ μm	3.3	6.5	0	0
	Composite[c]	$a^{-3.5}e^{-(0.0033a+0.437/a+50a^2)}$	1.55	105	26	0.45

[a] From MRN, with an extended size range $\{a_{\rm min}, a_{\rm max}\} = \{0.005\ \mu{\rm m}, 0.25\ \mu{\rm m}\}$.
[b] CFD, based on M96 and Dwek (1997).
[c] The CFD model contains amorphous carbon and silicates; for the size distribution $n(a)$, a is measured in microns.

can be found by measuring the extinction along the LOS. MCFK95 (and references therein) estimated the reddening $E(B-V)$ to be between 0.19 and 0.31 mag. Using the standard extinction law value of $R = 3.1$, this translated into a hydrogen column density in the range $N_{\rm H} = (1.1\text{–}1.8) \times 10^{21}$ cm^{-2}. There is a significant difference between the X-ray and extinction-derived hydrogen column densities. The former depends upon the source spectrum over a broad range of energies, whereas the latter depends on the source spectrum over a much narrower range (B and V bands) and provides a more direct measurement of the dust column density along the LOS. Therefore, like MCFK95, we adopt the extinction-determined hydrogen column density and use a value of $N_{\rm H} = 1.45 \times 10^{21}$ cm^{-2}. For the Nova Cygni source, MCFK95 noted that this column density creates only a small optical depth for scattering, so the assumption of single scattering is adequate. Nonetheless, the halo was clearly visible in the data to angles greater than 800″ before it merged with the background.

MCFK95 fit the halo using the RG approximation for the differential scattering cross section and found that an MRN model with a column density chosen to produce the observed visual extinction would scatter more X-rays than were seen. Noting that the intensity of the scattered light is proportional to the grain density squared, they proposed a model consisting of CFD particles with substantial amounts of vacuum that would scatter fewer X-rays but would nevertheless produce the same observed visual extinction. The amount of light scattered from a fluffy grain is less than that from the same size dense grain, since the fluffy grain has fewer electrons with which to scatter the X-rays. This reduction in scattering remains even when the total amount of mass in dust is constant, since the intensity is proportional to the number of electrons in each grain squared. Therefore, having twice as many grains that are 50% vacuum will lead to a net 50% drop in the intensity—when the RG approximation is valid.

In the 0.5 keV energy range, however, the RG approximation is not valid for dust grains larger than ~ 0.1 μm, for two reasons. First, the scattered waves will not add coherently, because the dust grain material will affect their phases substantially; secondly, absorption in the dust grain will remove some of the X-rays altogether. As a result, using the RG approximation with the no-damping Drude approximation to the optical constants will tend to substantially overpredict the amount of scattered light, and so the MCFK95 result must be reevaluated using the Mie solution.

To examine the robustness of the conclusions derived by MCFK95 for the Nova Cygni data, we modeled the same data using Mie theory for the standard MRN model and the newly proposed CFD model (M96). The parameters of the two models are presented in Table 1. The two dust models produce an overall equally good fit to the average interstellar extinction curve (Dwek 1997). However, the CFD model produces a visual extinction that is 6.7% higher than the MRN model, so we normalized the X-ray scattering intensity downward by the same amount. With this renormalization the two models produce the same amount of visual extinction toward the X-ray source. We limited our results to the case of evenly distributed dust, i.e., $f(z) \equiv 1$.

Our results are shown in Table 2 and Figure 7. These show the observed halo intensity, as well as the intensity calculated using the RG approximation and the Mie solution, for both the CFD and the MRN grain models. For both types of grains, the RG approximation overestimates the amount of scattering; in this case, neither the MRN nor the CFD models fitted the data. However, both models, when calculated using the Mie solution, predict similar amounts of scattering, which are slightly less than the

TABLE 2

NOVA CYGNI 1992 SCATTERING INTENSITY: DATA (FROM MCFK95) AND MODELS

θ (arcsec)	Observed (counts arcmin^{-2})	MRN RG (counts arcmin^{-2})	MRN Mie (counts arcmin^{-2})	Composite RG (counts arcmin^{-2})	Composite Mie (counts arcmin^{-2})
100.....	136 ± 15	137.7	43.2	100.5	42.9
200.....	34 ± 4	62.0	19.5	44.2	18.7
300.....	17 ± 2.5	36.9	11.6	25.7	10.9
400.....	13.4 ± 2.0	24.6	7.73	16.6	6.94
500.....	8.7 ± 1.2	17.3	5.45	11.3	4.68
600.....	5.5 ± 1.2	12.6	3.98	7.99	3.26
800.....	2.4 ± 0.8	7.14	2.27	4.19	1.73

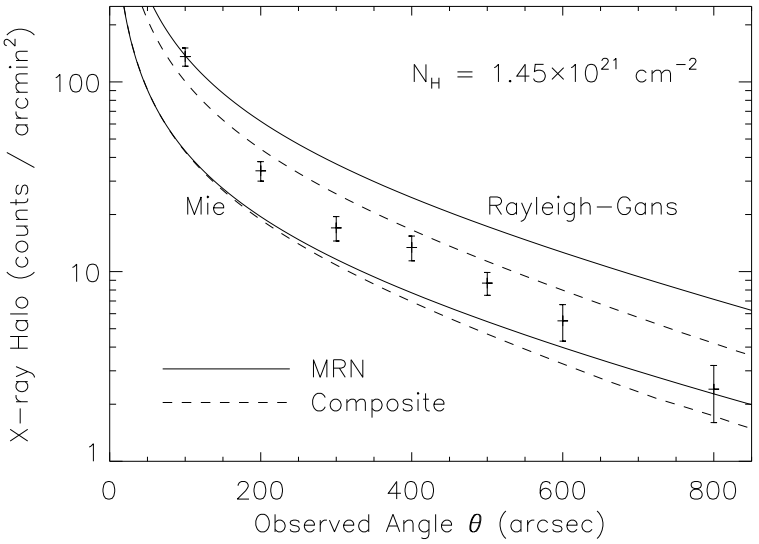


FIG. 7.—Nova Cygni 1992 data, with MRN (bare spherical silicate and graphite grains) and CFD models (M96). The RG approximation overestimates the amount of scatter in both cases, while the Mie solution underestimates the data, with similar results for either type of dust model. Unlike the RG approximation results, the Mie solution does not distinguish between fluffy and dense dust. This figure illustrates that the Nova Cygni 1992 data cannot be used to infer the morphology of the scattering dust.

observed scattering. While none of the four models fit the data particularly well, we can make some useful observations:

1. The fit depends on N_H. The measured column density was $N_H = (1.45 \pm 0.35) \times 10^{21}$ cm^{-2}. We use the central value, but using the upper 1 σ value would mean the Mie solution models fit the data well. To fit the RG approximation with fluffy dust requires the lower 1 σ value and an even larger value for the dense dust.

2. While there is a large difference between the fluffy and dense dust models in the RG solution, the difference is much smaller when using the Mie calculations. The likely reason for this is that, for a given dust size, absorption is more important for the dense dust than for the fluffy dust, and as a result the scattering from dense dust is reduced relative to fluffy dust. Therefore, we conclude that the Nova Cygni 1992 data does not distinguish between fluffy and dense dust.

Finally, it is important to note that while the Mie solution models marginally fit the data at larger angles, they substantially underestimate the observed scattering at 100″. At small observed angles θ, dust along the LOS in the vicinity of the source dominates the observed intensity. Therefore, the larger halo intensity seen at small angles may be due to an increased number of dust grains near the source.

5. CONCLUSIONS

X-ray scattering is a powerful tool for measuring the composition and size distribution of interstellar dust. However, many approximations and assumptions are necessary to create models of the data. We have assumed, for example, that dust grains are spherical, homogeneous, and evenly distributed throughout the ISM, assumptions whose effects should be tested. We have explored the use of the RG approximation for the differential scattering cross section, which, when combined with the Drude approximation to the index of refraction, provides a very convenient analytical form for discussing X-ray scattering. We find that the RG approximation works well for normal interstellar dust parameters and energies at or above 2 keV, but below this energy it overestimates the halo intensity.

We reexamined the Nova Cygni 1992 data, which has a strong X-ray halo, and found that it does not distinguish between fluffy and dense dust. Mie calculations using measured optical constants produce equally good fits for the standard MRN model and for fluffy dust particles. Consequently, the Nova Cygni data cannot be used as evidence that interstellar dust particles are fluffy, although they may be.

The future of X-ray scattering is bright. Although the *ROSAT* PSPC has the highest energy-resolved spatial resolution available currently, the *AXAF* CCD Imaging Spectrometer (ACIS) will have a much lower detector background and a tight point-response function with low to moderate energy resolution. Clearly, nearly every moderately absorbed point source seen with *AXAF* will include an X-ray halo of some kind. Observers will be able to detect halos only 10″ away from of the source, where the scattered intensity is due almost entirely to grains very near the source. This will be a bonanza for dust grain theorists, as it will provide a new handle on the size distribution of larger grains as well as the position-dependence of grain populations. At the same time it will add a difficulty to the data analysis of diffuse sources, since a calculation of the X-ray halo due to dust scattering will have to be made in order to remove it, in a process similar to the "dereddening" required of optical and UV measurements.

We would like to thank the referee, Chris Mauche, for his cogent and helpful comments on this work. We also thank Alain Léger for invoking our interest in this problem. This work was performed while one of the authors (R. K. S.) held a National Research Council-GSFC Research Associateship. This research was also supported by NASA Astrophysics Theory Program grant 344-02-05-01.

APPENDIX A

DERIVING THE HALO INTENSITY

Consider a dust particle of size a at a point P, illuminated by an X-ray source S a distance R_1 away, which scatters photons of energy E toward an observer O at a distance R_2, as is shown in Figure 1. Given a source luminosity of $L(E)$ (in photons s^{-1}), the flux at P is $L(E) \exp [-N_{\rm H}({\rm SP})\sigma(E)]/4\pi R_1^2$, where $N_{\rm H}({\rm SP})$ is the hydrogen column density along the line SP and $\sigma(E)$ is the average interstellar absorption cross section at energy E. Then the luminosity of photons scattered into solid angle $d\Omega$ is

$$L_{\rm sca}(E) = \frac{L(E) \exp [-\sigma(E)N_{\rm H}({\rm SP})]}{4\pi R_1^2} \left(\frac{d\sigma}{d\Omega}\right) d\Omega \, . \tag{A1}$$

Now consider the photons arriving at the observer, who measures the number of photons of energy E from the scattered dust particle, using a detector of size dA' and a telescope with opening angle $d\Omega'$. Then we can choose $d\Omega$ so that $dA' = R_2^2 \, d\Omega$, and the observer obtains a photon count rate of

$$C(E) = \frac{L(E) \exp [-\sigma(E)N_{\rm H}({\rm SP})]}{4\pi R_1^2} \left(\frac{d\sigma}{d\Omega}\right) \exp [-\sigma(E)N_{\rm H}({\rm PO})] \frac{dA'}{R_2^2} \, . \tag{A2}$$

This is the result for a single dust particle; we can now integrate it over all dust particles in the scattering volume. Assume that there are $n_g(P)$ dust grains per unit volume at position P. We will integrate over the LOS using a differential volume element with length dR_2 and solid angle $d\Omega'$. The volume is $dV = R_2^2 \, dR_2 \, d\Omega'$, and we obtain the total count rate by integrating over R_2:

$$\begin{aligned} C_{\rm tot}(E) &= \int \frac{L(E) \exp [-\sigma(E)N_{\rm H}({\rm SP})]}{4\pi R_1^2} \left(\frac{d\sigma}{d\Omega}\right) n_g(P) \exp [-\sigma(E)N_{\rm H}({\rm PO})] \frac{dA'}{R_2^2} \, R_2^2 \, dR_2 \, d\Omega' \\ &= dA' \, d\Omega' \int \frac{n_g(P)L(E) \exp \{-\sigma(E)[N_{\rm H}({\rm SP}) + N_{\rm H}({\rm PO})]\}}{4\pi R_1^2} \left(\frac{d\sigma}{d\Omega}\right) dR_2 \, . \end{aligned}$$

Thus the count rate (in photons per second) in a detector with area dA' and opening angle $d\Omega'$ is given by $C_{\rm tot}(E)$. We can therefore write the intensity of the scattered light as

$$I_{\rm sca}(E, a, \theta) = \int \frac{n_g(P)L(E) \exp \{-\sigma(E)[N_{\rm H}({\rm SP}) + N_{\rm H}({\rm PO})]\sigma(E)\}}{4\pi R_1^2} \left(\frac{d\sigma}{d\Omega}\right) dR_2 \, . \tag{A3}$$

This equation must then be integrated over a energy bandpass and a range of dust size and position distributions. In general, the function n_g will be a function of dust radius a as well as a function of position. Therefore, the total scattering for a given energy range (E_1, E_2) will be

$$I_{\rm sca}(\theta) = \int_{E_1}^{E_2} \int_{a_{\rm min}}^{a_{\rm max}} \int_0^D \frac{n_g(a, P)L(E) \exp \{-\sigma(E)[N_{\rm H}({\rm SP}) + N_{\rm H}({\rm PO})]\}}{4\pi R_1^2} \left(\frac{d\sigma}{d\Omega}\right) dR_2 \, da \, dE \, . \tag{A4}$$

This equation is completely general; however, we can simplify it substantially if the observed angle θ is very small, limiting the observations to very small angles. In this case, the path traveled by a scattered photon will be very close to that traveled by an unscattered photon, and the total hydrogen column density for the source, $N_{\rm H}(so)$, will be nearly the same as that of the scattered photons, $N_{\rm H}({\rm SP}) + N_{\rm H}({\rm PO})$. As a result, we have the following approximation:

$$\frac{L(E) \exp \{-\sigma(E)[N_{\rm H}({\rm SP}) + N_{\rm H}({\rm PO})]\}}{4\pi R_1^2} \approx \frac{F_{\rm X}(E) \cos (\phi - \theta)}{(1 - z)^2} \, , \tag{A5}$$

where $F_{\rm X}(E)$ is the observed flux from the source. We can then rewrite equation (A4) in terms of the normalized projected position coordinate z and the scattering angles θ and ϕ:

$$I_{\rm sca}(\theta) = \int_{E_1}^{E_2} \int_{a_{\rm min}}^{a_{\rm max}} \int_0^1 \frac{n_g(a, z, \theta)F_{\rm X}(E) \cos (\phi - \theta)}{(1 - z)^2} \left(\frac{d\sigma}{d\Omega}\right) \frac{D}{\cos \theta} \, dz \, da \, dE \, . \tag{A6}$$

We can reduce this further by assuming that the dust size and position distributions are independent of each other. Using the assumption of similar paths for the scattered and direct photons and assuming $\cos \theta \approx 1$, we can rewrite equation (A6) to get

$$I_{\rm sca}(\theta) = N_{\rm H} \int_{E_1}^{E_2} F_{\rm X}(E) \int_{a_{\rm min}}^{a_{\rm max}} n(a) \int_0^1 \frac{f(z) \cos (\phi - \theta)}{(1 - z)^2} \left[\frac{d\sigma(E, a, \phi)}{d\Omega}\right] dz \, da \, dE \, , \tag{A7}$$

where $f(z) \equiv n_{\rm H}(z)D/N_{\rm H}$, and $N_{\rm H}$ is the total hydrogen column density to the source. The final assumption necessary to derive equation (1) in the text is that $\cos (\phi - \theta) \approx 1$. We have already limited the observed angle θ to small angles. Although, close to the X-ray source, ϕ can be large, even for very small values of θ, $(d\sigma/d\Omega)$ is strongly suppressed at scattering angles above 1°, so that in practice all the contribution to the scattered light comes from scattering angles below 1°. Therefore, the actual

scattering angle ϕ will be small, so $\cos(\phi - \theta) \approx 1$. Note also that $\phi > \theta$ for all geometries. For a nonuniform dust distribution, in which a significant amount of dust is near the source, the contribution from larger scattering angles may be important, and an exact expression for $\cos(\phi - \theta)$ will then be required.

REFERENCES

Bohren, C. F., & Huffman, D. R. 1983, Absorption and Scattering of Light by Small Particles (New York: Wiley)
Canizares, C. R. 1990, Adv. Space Res., 10(2), 261
Cardelli, J. A., Meyer, D. N., Jura, M., & Savage, B. D. 1996, ApJ, 467, 334
Draine, B. T. 1988, ApJ, 333, 848
Draine, B. T., & Lee, H. M. 1984, ApJ, 285, 89
Dwek, E. 1997, ApJ, 484, 779
Dwek, E., & Smith, R. K. 1996, ApJ, 459, 686
Dwek, E., et al. 1997, ApJ, 475, 565
Glatter, O., & Kratky, O. 1982, Small-Angle X-Ray Scattering (London: Academic)
Henke, B. L. 1981, in Low-Energy X-Ray Diagnostics, ed. D. T. Attwood & B. L. Henke (New York: AIP)
Jackson, J. D. 1975, Classical Electrodynamics (2d ed.; New York: Wiley)
Martin, P. G., & Rouleau, F. 1991, in Extreme Ultraviolet Astronomy, ed. R. F. Malina & S. Bowyer (New York: Pergamon)
Mathis, J. S. 1990, AR&A, 28, 37
———. 1996, ApJ, 472, 643 (M96)
Mathis, J. S., Cohen, D., Finley, J. P., & Krautter, J. 1995, ApJ, 449, 320 (MCFK95)
Mathis, J. S., & Lee, C. W. 1991, ApJ, 376, 490 (ML91)
Mathis, J. S., Rumpl, W., & Nordsieck, K. H. 1977, ApJ, 217, 425 (MRN)
Mauche, C. W., & Gorenstein, P. 1986, ApJ, 302, 371 (MG86)
Overbeck, J. W. 1965, ApJ, 141, 864
Predehl, P. 1996, in MPE Report 263, Röntgenstrahlung from the Universe (Garching: MPE), 623
Predehl, P., & Klose, S. 1996, A&A, 306, 283 (PK96)
Predehl, P., & Schmitt, J. H. H. M. 1995, A&A, 246, L40
Rouleau, F., & Martin, P. G. 1991, ApJ, 377, 526
van de Hulst, H. C. 1957, Light Scattering by Small Particles (New York: Dover)
Wiscombe, W. 1979, NCAR Tech. Note TN-140+STR, Mie Scattering Calculations—Advances in Technique And Fast, Vector-Speed Computer Codes (Boulder: NCAR)
———. 1980, Appl. Opt., 19, 1505
Woo, J. W., Clark, G. W., Day, C. S. R., Nagase, F., & Takeshima, T. 1994, ApJ, 436, L5